An Investigation of Filter Choice for Filtered Back-Projection Reconstruction in PET

T. H. Farquhar, *Student Member, IEEE,* A. Chatziioannou, *Member, IEEE,* G. Chinn, *Member, IEEE,* M. Dahlbom, *Senior Member, IEEE,* and E. J. Hoffman, *Fellow, IEEE*

Division of Nuclear Medicine & Biophysics, Department of Medical and Molecular Pharmacology UCLA School of Medicine, Los Angeles, CA 90095

ABSTRACT

A key parameter in the practical application of filtered back-projection (FBP), the standard clinical image reconstruction algorithm for positron emission tomography (PET), is the choice of a low-pass filter window function and its cut-off frequency. However, the filter windows and cut-off frequencies for clinical reconstruction are usually chosen empirically, based on a small sample of images and filters. By considering the features of the signal and noise spectra in a sinogram, the desired image resolution, and the signal-to-noise ratio (SNR) of the filtered sinogram, a methodology for informed selection of a filter function and cut-off frequency for FBP was investigated. Simulations of sinogram data similar to whole body or cardiac studies provided information on the signal and noise frequency-domain spectra of noisy projection data. The improvements in SNR with different filter windows and cut-off frequencies were evaluated and compared. The projection spectrum SNR measure did not prove to be an accurate indicator of subjective image quality or lesion detectability with variations in Poisson noise and image resolution.

I. INTRODUCTION

The standard algorithm used for clinical image reconstruction in positron emission tomography (PET) is filtered back-projection (FBP). The data acquired in PET studies usually suffers from the presence of significant statistical noise. This condition is further exacerbated by the high frequency noise amplifying effect of the ramp reconstruction filter in FBP [1]. To reduce this high frequency noise in the reconstructed image, a low-pass windowing function is usually applied to the ramp reconstruction filter, and this combination is referred to as the filter.

Many filter functions have been suggested for use with FBP; most are windowing functions generally used in signal processing while others have been specifically designed for use in PET [2]. In general, a single parameter, a cut-off frequency F_C, is used to modify the frequency response for the filter function that has been chosen. The quality of a reconstructed image, in terms of noise, resolution, contrast and other measures, can vary greatly with the use of a different filter and cut-off frequency. A filter with a cut-off frequency that is too high may maintain resolution and contrast, but allow noise to degrade the reconstructed image quality. Conversely, a filter with too low of a cut-off frequency will suppress image noise, but may overly smooth the image, decrease contrast and eventually introduce ringing artifacts.

Currently, the filter functions for clinical reconstruction are generally chosen empirically, based on a relatively small sample of images and filters. Clearly, this empirical method is not optimal, and, furthermore, does not suggest any systematic method for choices of filter for applications which differ from the studies used to make the selection. Previous studies with the goal of selecting an optimal filter function for use with FBP in emission tomography have used lesion detectability as the metric to be optimized [3-6]. However, evaluating performance for lesion detection necessitates a time-consuming observer study, using ROC methodology [3] or alternatives such as a computer observer [4]. Furthermore, even after the extensive effort of an observer study, there is no guarantee that an optimal filter cut-off frequency will be indicated. Automated methods have been proposed which apply statistical tests to the object and noise power spectra in the projections, in order to ascertain the optimal cut-off frequency for a SPECT restoration filter [7].

Likewise, this study considered the possibility of using the signal and noise spectra in the projection data from simulations of a particular PET application (FDG scans of the thorax) to suggest an optimal low-pass linear windowing function. Accurate knowledge of the signal and noise power spectra would allow formulation of an optimal, linear, Wiener filter to give a minimum mean square error solution. However, implementation of a Wiener filter is complicated by the difficulty in precise determination of the power spectrum [8]. Therefore, this study did not focus on design of a new filter function, such as a Wiener filter. Instead, the effect of the frequency response of three commonly used filter functions (ramp, Shepp-Logan, Hann) on the signal and noise spectra of simulated projections is compared. The usefulness of a global measure of the signal-to-noise ratio (SNR) in the projection spectra was evaluated in relation to the reconstructed image resolution and total number of counts in the projection data. The overall aim is to ascertain if this simple measure can be used to select an advantageous window function and cut-off frequency, without the effort of an observer performance study.

This project was supported in part by NCI Grant R01-CA56655, DoE Contract DE-FC03-87-ER-60615, NIH NIGMS Training Grant GM08042, the UCLA Medical Scientist Training Program, and the Aesculapians' Fund of the UCLA School of Medicine.

0018-9499/98$10.00

II. METHODS

Simulations of sinograms for 2-D acquisitions with an ECAT EXACT HR 961 PET scanner (CTI, Inc., Knoxville, TN) were performed for different noise levels. The simulations included the effects of Poisson noise, photon attenuation, detector efficiencies, and line spread function. The simulated phantom is depicted in Fig. 1. The small sample spacing (1.65 mm) and large number of samples per projection (336 samples/projection) in the EXACT HR is beneficial because the computed projection frequency spectrum will have a higher maximum spatial frequency and more frequency domain samples. The Nyquist frequency for HR 961 projections is 3.03 cycles/cm. The frequency spectrum for each projection in a sinogram was determined in the following manner: (1) the simulated sinogram is normalized and corrected for attenuation; (2) the discrete Fourier transform is calculated for each projection in the sinogram; (3) the magnitude of the complex values in the spatial frequency spectrum are summed over all angles in the sinogram. Summing over the angles does not account for the variation in the projections with angle, but the resulting envelope is still a useful measure. Furthermore, the spatial frequency spectrum is not seen to change greatly when no attenuation correction is applied. The noise spectrum is estimated as the difference between noisy and noiseless spectra for simulations where the spectrum was calculated with and without Poisson noise. The SNR versus spatial frequency is calculated by dividing the magnitude of the signal content by the noise content for each frequency bin.

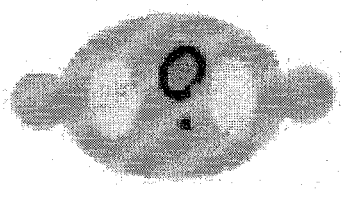

FIG. 1. Thorax phantom used in simulations of sinogram signal and noise spectra, consisting of: lungs, myocardium with defect, tumor, and background activity.

The reconstructed image resolution for each filter with a range of cut-off frequencies was determined by measurement with a Na-22 line source positioned approximately at the center of an HR 961 scanner. After reconstruction with each of the filters with different cut-off frequencies, the full width half maximum (FWHM) was determined using radial and tangential profiles through the source. This measured FWHM is used as the metric of resolution.

III. RESULTS

The signal spectrum for different parts of the simulation phantom, with and without noise, are shown in Fig. 2. As expected, the majority of the signal content is in the lower spatial frequencies, with a rapid drop-off before 1.2 cycles/cm (0.4 of Nyquist), while the noise dominates the higher frequencies. Moreover, the effect of object size on the projection spectrum can be seen: the signal strength tapers rapidly with increasing spatial frequency for larger objects, and more slowly for smaller ones (such as the tumor). If the noise is large even at lower frequencies, from approximately 0.3 - 0.9 cycles/cm (0.1 to 0.3 of Nyquist), features of the signal spectrum will be hidden. Fig. 3 illustrates noise obscuring the signal spectrum from an actual dynamic acquisition of a thorax phantom with an HR 961 system. As

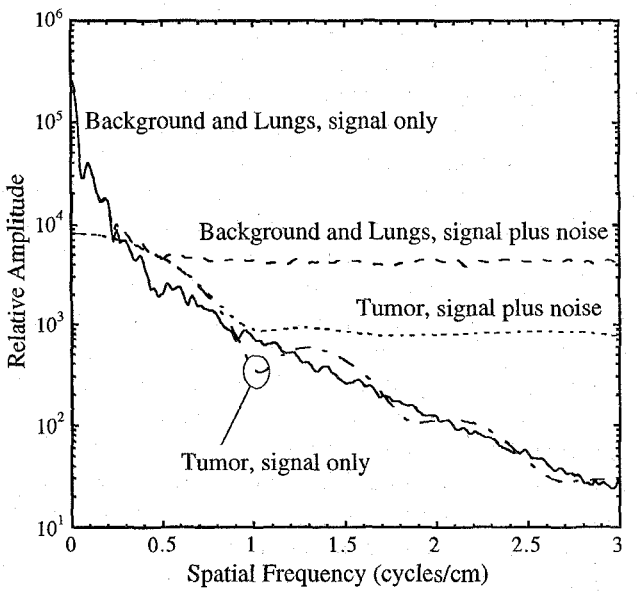

FIG. 2. Simulated projection spectra for parts of the thorax phantom. The parts depicted are the background activity and lungs, and the tumor. Each was simulated with and without Poisson noise.

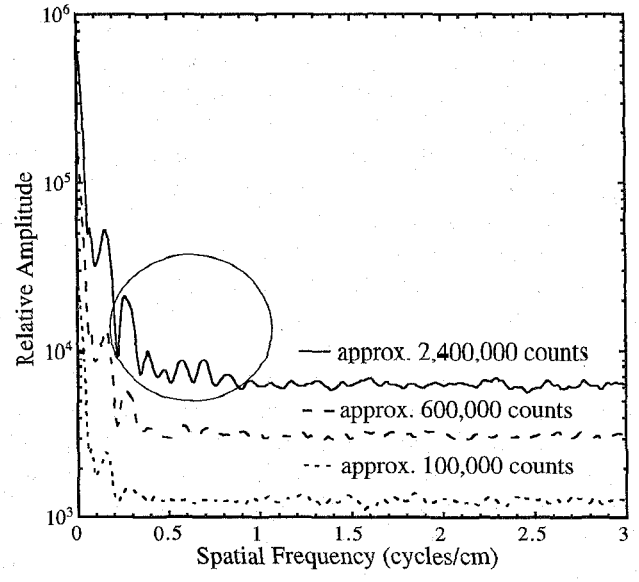

FIG. 3. Sinogram spectrum from dynamic acquisition of thorax phantom. The spectra for sinogram data with 100,000 counts, 600,000 counts, and 2.4 million counts are shown. Features of the underlying signal spectrum that become evident as the count level increases are highlighted in the oval.

the number of counts is increased from 100,000 to 2.4 million, features of the underlying signal spectrum become evident as the relative noise power decreases. This estimation of the signal content establishes a minimum cut-off frequency to prevent loss of crucial image features. Fig. 3. would suggest that the signal strength may be significant compared to the noise content for spatial frequencies of up to 0.75 cycles/cm (0.25 of Nyquist), but only for high count studies.

The resolution for each filter and cut-off frequency is shown in Fig. 4. The SNR characteristics of filters are compared by matching resolution, rather than comparison by cut-off frequency. Once the optimal resolution is determined, the cut-off frequency can be inferred.

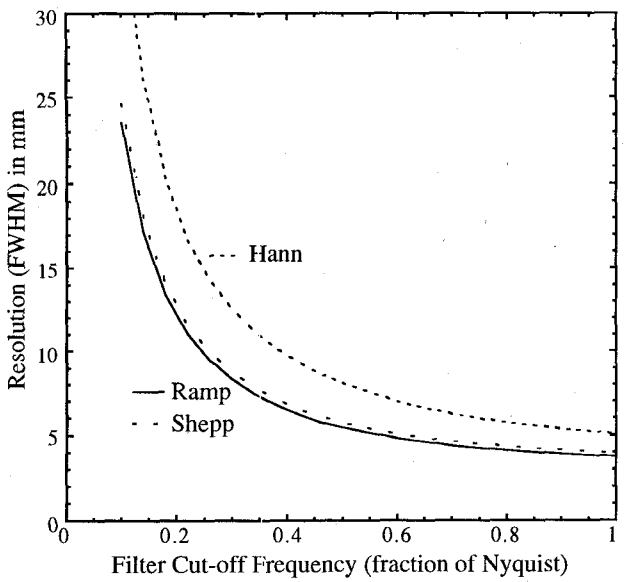

FIG. 4. Measured resolution as FWHM from reconstructed image for different filters and cut-off frequencies.

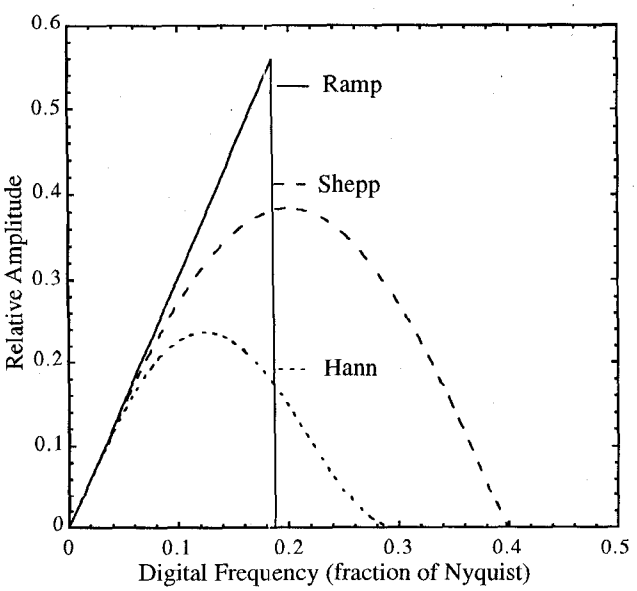

FIG. 5. Frequency response of ramp, Shepp-Logan, and Hann filter functions all with 12.5 mm FWHM resolution.

The difference in the frequency response of the three linear filter functions considered is evident in Fig. 5. In each case, the cut-off frequency was chosen to give equivalent resolution as measured by the FWHM. Filtering has a beneficial effect on the overall SNR because it removes predominately noise power at the higher frequencies. By summing the total signal and noise power after filtering in each frequency bin of the spectrum, a post-filtering SNR measure can be obtained for each particular filter and cut-off frequency. The noise spectrum will vary with the noise level (number of counts) in a simulation, so it is possible to generate a family of curves. Fig. 6 depicts such a family of curves, with increasing count levels from 100,000 counts to 200,000 counts (approximately equivalent to a typical whole body or cardiac study) to 20 million counts. As expected, the SNR increases as more smoothing is applied with the filter, i.e. larger resolution elements. Also of interest is the shape of the curves. For higher count levels, the beginning of the curve is steeper, and the latter portion flatter. Thus, smoothing can initially result in significant increases in SNR, but additional smoothing will have decreased effectiveness.

The measurements of the projection spectrum SNR performed to obtain Fig. 6 were repeated with the signal spectrum from the tumor alone used in place of the signal spectrum from the entire phantom. The noise spectrum remained unchanged with noise contributed by all of the components of the phantom (background, heart, etc.). These results are compared in Fig. 7. This alternative measure was considered because the tumor will be the most important signal in clinical interpretation of the image. Therefore, this second measure was used to decide if the tumor-only projection spectrum SNR showed more sensitivity to changes in the filter frequency response than a projection

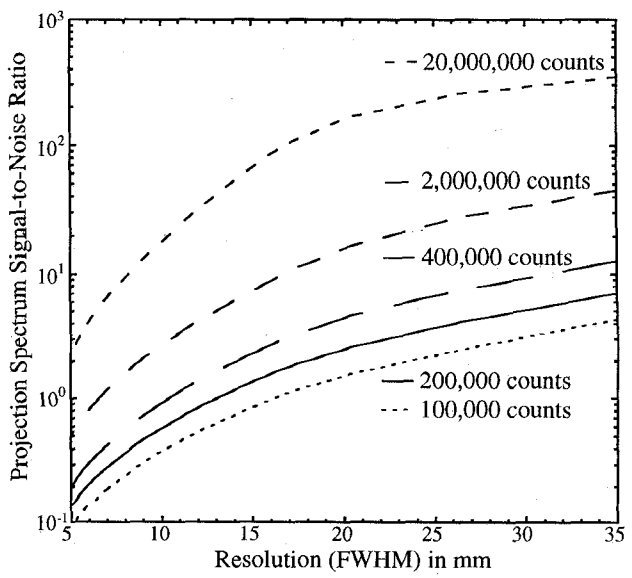

FIG. 6. Projection spectrum SNR versus resolution for different count levels. The filter used was a ramp filter with a Hann window.

spectrum SNR which used signal from all components of the phantom. Fig. 7 indicates that either method for computing the projection spectrum SNR yields curves with similar shape. As expected, the tumor-only projection spectrum SNR (dashed lines) have reduced SNR at all frequencies, because the signal from other components of the phantom has been removed but the noise from those components remains. After considering this global reduction in SNR, there is a relative increase in SNR for better resolution with a relative decrease as the resolution worsens. This trend is expected because the tumor-only signal has greater signal strength at high frequencies, compared to the signal spectrum of the entire phantom, as shown in Fig. 2.

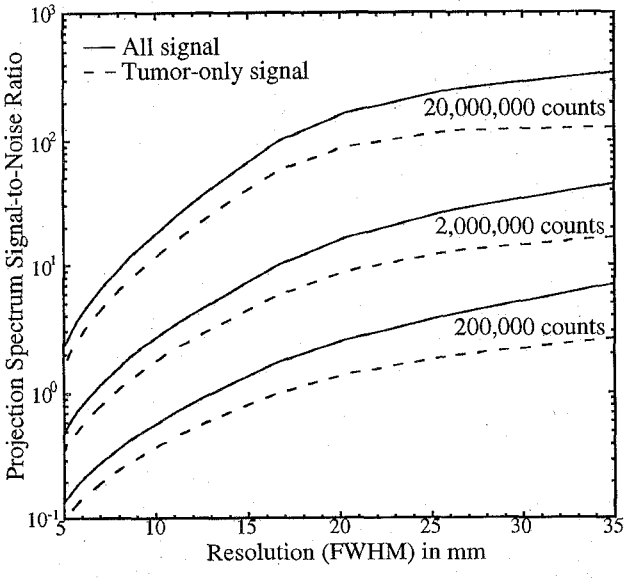

FIG. 7. Projection spectrum SNR versus resolution for different count levels, using the signal from the entire phantom (solid lines) or the signal from only the tumor (dashed lines). The filter used was a ramp filter with a Hann window.

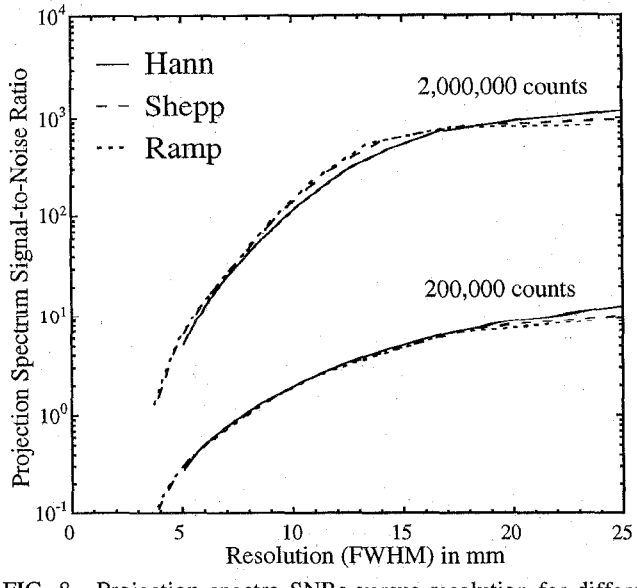

FIG. 8. Projection spectra SNRs versus resolution for different filters at two count levels. The bottom set of curves is for a simulation of 200,000 counts/plane (roughly equivalent to a whole body or cardiac study). The top set of curves is for 2 million counts/plane.

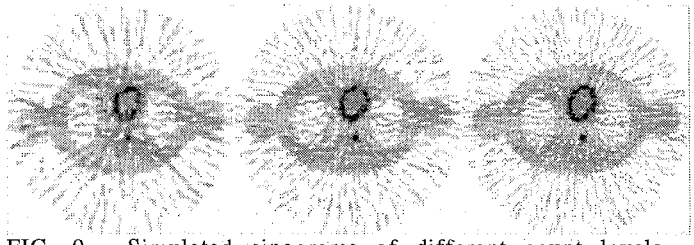

FIG. 9. Simulated sinograms of different count levels reconstructed to equivalent spectral signal-to-noise levels. Left: 100,000 counts reconstructed to 15.4 mm resolution. Middle: 200,000 counts reconstructed to 12.6 mm resolution (equivalent to clinical study). Right: 400,000 counts reconstructed to 9.9 mm resolution. In each case, the calculated projection spectrum SNR is approximately 1.7.

Fig. 8 shows projection spectrum SNR curves, using the signal spectrum from all of the phantom components, for three different filters, at two noise levels. In both cases, on the basis of the simulations, it is apparent that the SNR from the projection spectrum is predominately dependent on the resolution of the filter and cut-off frequency chosen, and does not vary greatly with the specific form of the filter.

To evaluate a possible relationship between the predicted SNR for a chosen filter function calculated using this simulation method, the number of counts in a sinogram, and the subjective reconstructed image quality, images reconstructed from simulated sinograms of three count levels were compared. These images are shown in Fig. 9. The low-count image, with only 100,000 counts per plane, was reconstructed with a filter to a final image resolution of 15.4 mm FWHM. The intermediate image was taken from a sinogram with 200,000 counts per plane using the clinical reconstruction filter which gives a final image resolution of 12.6 mm FWHM; according to the simulations and analysis, this should represent a similar spectral SNR to the 100,00 count image. The parameters of the intermediate reconstructed image represent the current, typical clinical protocol in terms of filter choice and acquired sinogram counts. Lastly, a high-count image, with 400,000 counts per plane was reconstructed to a final image resolution of 9.9 mm FWHM. Again, this should be an equivalent SNR according to Fig. 6.

IV. Discussion

The simple SNR measure described, computed from simulated projection spectra, indicated neither an optimal choice of filter function nor an optimal cut-off frequency for the filter functions. The SNR increases monotonically with continued smoothing and worsened resolution, without reaching a local maximum; thus, no preferred operating point on the SNR vs. resolution curves is suggested. For count levels closer to those usually seen with the acquisition protocol times and isotope doses of current whole body and cardiac protocols, the SNR rises steadily with increased

image smoothing. Only the introduction of severe blurring and artifacts at very low cut-off frequencies sets a bound to the advantage of increased smoothing.

The noticeable difference in image quality between the images of Fig. 9 further suggest that this SNR measure is not suitable to predict subjective image quality with variations in count levels and image resolution. It is unlikely that this method would be dramatically improved through more accurate simulation, for example including random coincidences or the effects of axial smoothing. Moreover, the relationship between the projection spectrum SNR and the SNR at a region-of-interest in the image is difficult to assess, because frequency components in the projection spectrum contribute to all pixels in the image, but with varying strength.

However, the results of this study, particularly the trends seen in Fig. 8, do suggest that a linear filter for FBP reconstruction of PET images can be chosen on the basis of the desired resolution alone. Despite the differences in the frequency response spectra for each filter, as seen in Fig. 5, the particular choice of a filter function does not seem to dramatically alter the SNR or image quality because of the signal spectrum of a typical PET sinogram. As seen in Fig. 2, the vast majority of the signal power is seen at frequencies well below 0.6 cycles/cm (0.2 of Nyquist). Using a filter which rolls off much below 0.6 cycles/cm (0.2 of Nyquist) severely degrades the resolution (>> 15 mm as shown in Fig. 6), so a filter that severe is not desirable. Thus, regardless of the choice of windowing function, the filter will be very close to a ramp at the frequencies with the majority of the signal power. These results also indicate that if linear filtering methods are used, filtering in the sinogram and image domains should be identical, with no benefit to smoothing the data prior to reconstruction.

The results of this study and the work of others [3-7] suggest that the current clinical method of empirically choosing the filter function and cut-off frequency for FBP reconstruction of PET images is most likely fairly robust. It is likely that the diagnostic image quality remains relatively unchanged after a sufficient initial degree of smoothing; the noise reduction from further smoothing is likely offset by the degradation in resolution and contrast. This projection spectrum SNR measure is not a suitable model for addressing optimization of the complex task of diagnostic image interpretation.

V. Conclusion

It is well established that smoothing the noisy projection data of PET sinograms with a linear, low-pass windowing function during reconstruction with FBP will enhance the subjective image quality and usefulness of the image for tasks such as lesion detection. The signal and noise spectra of simulated sinograms for cardiac and whole body PET studies were analyzed and the post-filtering projection signal-to-noise ratio was compared. The post-filtering projection spectrum SNRs showed little difference despite the different frequency response characteristics of the three window functions used (ramp, Hann, and Shepp-Logan), when the filters were matched for image resolution. Unfortunately, because of the complex variation of image quality with count level, image resolution, isotope distribution and/or object shape, examination of the signal and noise projection spectra characteristics is not well suited to objective selection of an optimal filter function and cut-off frequency. This simple, objective method, therefore, cannot be considered a suitable replacement to an observer performance study.

References

[1] M. E. Phelps, S.-C. Huang, E. J. Hoffman, D. Plummer, and R. Carson, "An analysis of signal amplification using small detectors in positron emission tomography," *Journal of Computer Assisted Tomography*, vol. 6, pp. 551-65, 1982.

[2] L. A. Shepp and B. F. Logan, "The Fourier reconstruction of a head section," *IEEE Transactions on Nuclear Science*, vol. 21, pp. 21-43, 1974.

[3] D. R. Gilland, B. M. W. Tsui, W. H. McCartney, J. R. Perry, and J. Berg, "Determination of the optimum filter function for SPECT imaging," *Journal of Nuclear Medicine*, vol. 29, pp. 643-50, 1988.

[4] M. T. Chan, R. M. Leahy, E. U. Mumcouglu, S. R. Cherry, J. Czernin, and A. Chatziioannou, "Comparing lesion detection performance for PET image reconstruction algorithms: a case study," *IEEE Transactions on Nuclear Science*, vol. 44, pp. 1558-63, 1997.

[5] J. H. Kim, K. I. Kim, and C. E. Kwark, "A filter design for optimization of lesion detection in SPECT," *1996 IEEE Nuclear Science Symposium Conference Record*, pp. 1683-7, 1996.

[6] H.-G. Liu, J. M. Harris, C. S. Inampudi, and J. M. Mountz, "Optimal reconstruction filter parameters for multi-headed brain SPECT: dependence on count activity," *Journal of Nuclear Medicine Technology*, vol. 23, pp. 251-7, 1995.

[7] J. S. Beis, A. Celler, and J. S. Barney, "An automatic method to determine cutoff frequency based on image power spectrum," *IEEE Transactions on Nuclear Science*, vol. 42, pp. 2250-4, 1995.

[8] W. Y. Sun, T. F. Budinger, J. Llacer, and S. E. Derenzo, "Power spectra estimation for an adaptive Wiener filter reconstruction," *Journal of Nuclear Medicine*, vol. 34, pp. 184P, 1993.